

Design of an Electrocardiogram System for Physical Fitness Analysis using Heart Rate Variability and Maximal Oxygen Volume

Jana Utama^{1*}, Yeffry Handoko², Candra Saefulloh³

¹ Department of Electrical Engineering
Universitas Komputer Indonesia, Bandung, Indonesia
jana.utama@email.unikom.ac.id

² Department of Electrical Engineering
Universitas Komputer Indonesia, Bandung, Indonesia
yeffryhandoko@email.unikom.ac.id

³ Department of Electrical Engineering
Universitas Komputer Indonesia, Bandung, Indonesia
candrasaefulloh316@gmail.com

^{*}jana.utama@email.unikom.ac.id

ARTICLE INFO

Article history:

Received 11 August 2025

Accepted 21 October 2025

Published 05 November 2025

ABSTRACT IN ENGLISH

This study proposes a novel, low-cost, and portable real-time ECG monitoring system integrating the AD8232 sensor and Arduino Nano for comprehensive heart rate variability (HRV) assessment. Unlike conventional ECG devices, the proposed system combines affordable hardware with an embedded processing algorithm capable of directly calculating key time-domain HRV parameters—RMSSD, SDNN, NN50, pNN50, and VO₂Max—without the need for high-end laboratory equipment. The primary objective is to develop and validate a system that can accurately capture physiological responses during both resting and active conditions, enabling fitness assessment and potential early cardiovascular risk detection in field applications. The system was tested on five healthy subjects aged 20–22 years, demonstrating stable operation for over 40 minutes. Results showed that the average heart rate (HR) increased by **6.56% \pm 4.8%** from rest to activity, with the largest increase in Subject 1 (+12.09%) and the smallest in Subject 3 (+0.93%). Resting RMSSD values ranged from **75.36 to 99.76 ms**, decreasing on average by **6.21% \pm 4.7%** during activity. SDNN values ranged from **62.18–131.88 ms**, with Subject 2 showing an increase (122.33→129.06 ms) and Subject 5 a significant decrease (131.88→88.48 ms). NN50 at rest reached a maximum of **124 counts** (pNN50=77.78%) and a minimum of **23 counts** (pNN50=27%), with an average pNN50 reduction of **-18.42% \pm 21.5%** during activity; the largest drop occurred in Subject 5 (-54.64%), while Subject 1 increased (+26.07%). VO₂Max ranged from **29.98 ml/kg/min (poor)** to **39.90 ml/kg/min (excellent)**, correlating with HRV trends. These findings confirm that the system can quantitatively differentiate autonomic responses between individuals, highlighting its potential for real-time, on-site physiological monitoring, fitness evaluation, and early detection of abnormal cardiovascular patterns.

Keywords:

ECG; Heart Rate Variability;
VO₂Max; Arduino;
Software Processing 4

This is an open access article under the [CC BY-NC-SA](#) license.



1. INTRODUCTION

Coronary heart disease (CHD) remains one of the leading causes of death globally. Data from RSU Haji Surabaya indicate that hypertension and diabetes mellitus are the primary risk factors contributing to the high prevalence of CHD. This condition is caused by the buildup of fatty plaques in the coronary arteries, which restricts blood flow to the heart [1]. In Indonesia, the prevalence of CHD increased from 0.5% in 2013 to 1.5% in 2018, based on Riskesdas data. Research from the Subang Regional Hospital shows a significant correlation between high cholesterol and coronary heart disease (CHD), which is caused by unhealthy lifestyle habits [2]. An ideal health monitoring system typically emphasizes not only accuracy but also portability and efficiency. Research by Zen et al. demonstrated that the use of Long Short-Term Memory (LSTM) architecture on the Raspberry Pi allows for real-time heart rate detection with up to 96.66% accuracy, making it a practical solution for individual health monitoring [3]. Another study, by Akbar et al., stated that a real-time heart rate monitoring system must consider device portability, signal accuracy, and reliable connectivity [4].

Several related studies have explored various portable heart monitoring solutions. H. Nissa and A. S. Rachman used the AD8232 sensor to read heart rhythms. This sensor was chosen for its ability to detect the heart's electrical signals with high accuracy [5]. Another study by Sangeetha Lakshmi et al. utilized a cloud platform to store patient health data, allowing medical personnel to access patient data from multiple locations and conduct analysis for early detection of deteriorating health conditions [6].

Elmi Ramlan Bugis et al. proposed a portable heart rate monitor using the MAX30102 PPG sensor. Although the system recorded an average error of only 2.61%, its accuracy was affected by user movement, highlighting the need for improved stability and motion tolerance [7]. Royan et al. evaluated the accuracy of the AD8232 ECG sensor at various amplitudes and BPM levels using the ECP1202 simulator. Although the sensor performed accurately at higher amplitudes, it failed to detect signals at 0.5 mV, indirectly demonstrating its limitations in low-signal conditions [8]. Dange et al. also developed an ECG monitoring system using the AD8232 and Wi-Fi ESP8266, capable of transmitting accurate heart rate data [9]. Similarly, Pamungkas used the AD8232 sensor to record ECG signals and the MAX30102 sensor to measure heart rate and blood oxygen levels [10]. Recent studies have also highlighted the potential of low-cost health monitoring devices that integrate ECG and HRV analysis, showing promising accuracy while maintaining affordability and portability [11].

Previous studies have shown that most portable monitoring systems (i) lack advanced analytics beyond simple heart rate detection, (ii) are susceptible to motion artifacts and noise, or (iii) rely heavily on continuous internet connectivity, which reduces their practicality in certain settings. To address these limitations, this study proposes a portable ECG monitoring system using an AD8232 sensor and an Arduino Nano, with serial transmission to a laptop for further processing. The processing software not only visualizes the ECG waveform in real time but also performs Heart Rate Variability (HRV) analysis [12], R-R interval plots, Poincaré mapping [13], and estimation of maximal oxygen uptake (VO₂Max) [14], [15], providing a more comprehensive assessment of cardiovascular health and physical fitness compared to previous approaches.

The advantages of this proposed system are:

1. Enhanced analytical capabilities – unlike previous studies limited to BPM or ECG visualization, our system integrates HRV, Poincaré plots, and VO₂Max estimation for broader clinical and fitness evaluation.
2. Low-cost and portable hardware – the use of an Arduino Nano and AD8232 ensures affordability and ease of implementation compared to more complex IoT or Raspberry Pi solutions.
3. Offline operability with optional connectivity – the system can function without internet access, enhancing its applicability in remote or resource-constrained environments.

The remainder of this paper is organized as follows. Section 2 presents the methodology and system design. Section 3 discusses the results and their implications, including threats to validity. Finally, Section 4 concludes the study by summarizing the key contributions and suggesting potential directions for future research.

2. METHOD

Several studies have reported important limitations in the development of portable ECG monitoring systems. For example, some approaches rely heavily on stable internet connections for real-time functionality [6], [10]. Others tend to suffer from motion-related artifacts, which reduce measurement accuracy [7], [8]. In addition, many existing designs remain confined to basic BPM visualization and do not provide more advanced physiological metrics [5], [9]. In response to these shortcomings, this study proposes a low-cost and portable solution built on the Arduino Nano and AD8232 sensor, combined with bandpass and moving average filtering for improved signal quality. Beyond simple ECG display, the system introduces extended analytical features, including HRV assessment, Poincaré mapping, and VO₂Max estimation. The following subsections describe the methodology in detail.

2.1. Electrocardiogram (ECG)

An electrocardiogram (ECG) is a diagnostic method that records the heart's electrical activity that occurs during the depolarization and repolarization of the heart muscle during each heartbeat cycle [16]. This non-invasive device works by detecting changes in electrical potential through electrodes placed on the skin surface, such as those on the chest, wrist, and ankle. These electrical signals are then translated into a graphical form known as an electrocardiogram. In clinical practice, the ECG plays a crucial role in detecting various cardiovascular disorders, including arrhythmias, coronary artery disease, and myocardial infarction, which are indicated by characteristic abnormalities in the waveform [17].

A standard ECG consists of three main components: the P wave, the QRS complex, and the T wave, each of which represents a different electrical event in the cardiac cycle. The P wave reflects atrial depolarization, the QRS complex represents ventricular depolarization, which triggers contraction to pump blood out of the heart [18], and the T wave represents ventricular repolarization as it returns to its resting state. Changes in the duration, amplitude, or morphology of these components often indicate pathological abnormalities. For example, a prolonged QRS complex duration may indicate a conduction system abnormality, while ST-segment elevation is a hallmark of an acute heart attack.

The advantage of the ECG lies in its non-invasive, rapid, and relatively inexpensive nature, making it widely used for both diagnosis and monitoring. In addition to diagnosing heart disease, the ECG also serves to assess disease progression and monitor the effects of drug therapy. In emergencies, the ECG allows early detection of myocardial damage so that medical intervention can be initiated promptly. Routine screening is also beneficial for individuals with risk factors such as hypertension, diabetes, or a family history of heart disease.

In sports medicine, the ECG plays a crucial role in pre-participation screenings to ensure the heart condition of athletes before engaging in high-intensity activities [19]. Technological advances have also led to the emergence of portable, microcontroller-based ECG devices, such as the Arduino Nano combined with the AD8232 sensor, enabling more affordable heart health monitoring for personal and small clinic use [11], [20].

However, interpreting ECG results requires specialized expertise, and signal quality can be affected by electrode placement, patient movement, and electrical interference that can potentially cause artifacts. Despite these limitations, the ECG remains one of the most essential cardiovascular examination tools. Recent technological developments in hardware and signal processing are expected to further improve accuracy and accessibility, thus supporting early detection efforts and proactive monitoring of heart health [21].

2.2. Heart rate variability (HRV)

Heart rate variability (HRV) refers to the variation in the time interval between heartbeats, recorded through an ECG signal. HRV reflects the balance between the sympathetic nervous system, which increases heart rate during stress or physical activity, and the parasympathetic nervous system, which decreases heart rate for relaxation [12].

In time-domain analysis, one important parameter is the SDNN, with normal values in healthy populations generally >100 ms [22]. Other frequently used parameters are RMSSD (>25 ms) and pNN50 ($>3\%$) as indicators of autonomic balance [23]. Factors such as age, gender, fitness level, measurement time, and body position can influence HRV results [24]. A normal resting heart rate in healthy individuals ranges from 60–100 BPM with an R-R interval of approximately 0.6–1.2 s [25]. Therefore, HRV interpretation should be combined with other clinical and physiological parameters to obtain a more complete picture of cardiovascular health.

HRV has widespread applications in medicine and sports. In medicine, HRV is used to monitor patients' clinical conditions, detect fatigue, and evaluate the effectiveness of lifestyle interventions and medical therapies. In sports, HRV helps monitor fitness levels, training readiness, and injury risk. Athletes with high HRV generally have better recovery capacity than individuals with low HRV.

2.3. Maximum Oxygen Volume (VO₂Max)

Maximum Oxygen Volume (VO₂Max) represents the highest rate of oxygen consumption attainable during maximal exercise, measured in milliliters of oxygen per kilogram of body weight per minute (ml/kg/min). This critical physiological parameter serves as the gold standard for assessing an individual's aerobic capacity and cardiovascular endurance. Higher VO₂Max values indicate superior oxygen delivery and utilization by working muscles, which directly correlates with enhanced endurance performance in activities like distance running, cycling, and swimming. The average sedentary adult typically exhibits VO₂Max values between 30–45 ml/kg/min, while elite endurance athletes often surpass 70 ml/kg/min [26]. Cardiac rehabilitation programs frequently employ VO₂Max measurements to establish safe exercise thresholds and monitor patient progress [27]. Multiple factors influence VO₂Max, including both unmodifiable and modifiable elements. Genetic predisposition accounts for approximately 50% of an individual's VO₂Max potential,

establishing an upper limit that training cannot exceed. Age-related decline begins in the late 20s, with VO₂Max decreasing about 1% per year, primarily due to reduced cardiovascular efficiency and muscle mass. Gender differences are evident, with males generally displaying 15-30% higher values than females, largely attributable to greater muscle mass, higher hemoglobin levels, and larger heart size. Body composition plays a significant role as muscle tissue consumes substantially more oxygen than fat tissue during exercise. Among modifiable factors, regular aerobic training can increase VO₂Max by 15-20% through physiological adaptations including increased stroke volume, enhanced capillary density, and improved mitochondrial function [28]. Resistance training, such as running, swimming, and cycling, is known to significantly increase VO₂Max [29].

Accurate VO₂Max assessment typically requires laboratory-based maximal exercise testing using treadmill or cycle ergometer protocols with direct analysis of respiratory gases. These tests involve progressively increasing exercise intensity until volitional exhaustion while measuring oxygen consumption and carbon dioxide production. Although considered the gold standard, such testing requires specialized equipment and trained personnel. Practical alternatives include field tests like the 12-minute Cooper run, where the distance covered predicts VO₂Max, or the multistage 20-meter shuttle run (Balke test) [30][31]. While these field methods show strong correlations ($r=0.70-0.90$) with laboratory measures, they may underestimate true VO₂Max by 5-15% in trained individuals [31]. VO₂Max holds significant clinical and performance applications across multiple domains. In sports medicine, it serves as a primary determinant of endurance capacity, with values above 60 ml/kg/min typically required for competitive endurance athletes [24]. Clinically, VO₂Max provides powerful prognostic information, where values below 18 ml/kg/min indicate severe cardiovascular risk and impaired functional capacity [26]. Emerging research demonstrates that each 3.5 ml/kg/min increase in VO₂Max corresponds to approximately a 10-15% reduction in all-cause mortality, highlighting its importance as a health biomarker [32]. Furthermore, longitudinal studies suggest that maintaining VO₂Max through regular exercise may delay age-related physiological decline by 5-8 years [32]. The comprehensive assessment of VO₂Max integrates multiple physiological systems, reflecting the integrated function of pulmonary, cardiovascular, and muscular systems. As such, it remains one of the most valuable metrics in exercise physiology, sports performance, and preventive medicine. Current evidence strongly supports regular aerobic exercise as the most effective intervention for preserving and enhancing VO₂Max across the lifespan, with significant implications for both athletic performance and long-term health outcomes [26].

2.4. Bandpass Filter

A Bandpass Filter (BPF) is an essential signal processing component in Electrocardiogram (ECG) systems that selectively allows signals within a specific frequency range to pass while attenuating unwanted frequencies. This filter plays a critical role in isolating the QRS complex from background noise, P and T waves, and other artifacts that may interfere with ECG analysis [33]. The BPF combines both high-pass and low-pass filter characteristics, where the high-pass filter eliminates low-frequency noise (such as baseline wander and respiratory artifacts), and the low-pass filter suppresses high-frequency interference (including electrical noise and muscle activity).

The American Heart Association (AHA) recommends an optimal cutoff frequency range of 0.05 Hz to 150 Hz for ECG signal processing [34]. This range preserves all clinically relevant cardiac signal components while minimizing waveform distortion. Digital implementations commonly employ Butterworth filters due to their smooth frequency response and minimal phase distortion. Research indicates that a BPF with an 8-20 Hz frequency range significantly improves the signal-to-noise ratio (SNR), particularly for R-wave detection in motion-corrupted ECG signals [33]. However, improper filter selection can lead to diagnostic errors. For instance, using a high-pass filter with a 0.5 Hz cutoff may distort the ST segment, potentially causing misinterpretation of ischemic conditions. Thus, real-time monitoring systems should implement a 0.05 Hz high-pass cutoff to maintain waveform fidelity [34].

2.5. Moving Average Filter

The moving average (MA) filter is a straightforward yet effective approach in signal processing, where each point in the sequence is replaced by the mean of its neighboring samples. When applied to ECG signals, the MA filter can suppress random fluctuations and electrical noise, producing a waveform that is easier to interpret, particularly in the identification of the QRS complex. Instead of altering the morphology of the ECG, this smoothing method preserves the essential peaks while reducing small irregularities caused by electrode motion or baseline interference. Recent studies have shown that using an averaging window of around 26 samples provides a good balance between noise suppression and waveform clarity, thereby improving the accuracy of R-peak detection, which serves as the primary reference in heart rate estimation [35], [36].

2.6. Noise Filtering

In this research, several methods are used to eliminate noise in Electrocardiogram (ECG) signals to produce more accurate and stable data. Noise commonly found in ECG signals can come from electrical interference, electrode movement, muscle noise (EMG), and baseline disturbances. To address these issues, this system uses a combination of built-in filters from the AD8232 sensor along with two additional methods: Bandpass Filter (BPF) and Moving Average Filter (MA).

2.7. Built-in Filters of AD8232 Sensor

The AD8232 sensor is equipped with a High-Pass Filter (HPF) and Low-Pass Filter (LPF) to eliminate noise before the signal is sent to the Arduino Nano. These built-in filters help reduce baseline disturbances and unnecessary high frequencies.

AD8232 sensor specifications:

- a. Operating Voltage: 2.0V - 3.3V DC
- b. Current Consumption: 170 μ A
- c. Frequency Response: 0.5 Hz - 40 Hz
- d. Gain: ~100x (40 dB)
- e. Filters: High-Pass & Low-Pass.

The AD8232 sensor uses a High-Pass Filter (HPF) to eliminate low-frequency noise, such as baseline drift caused by electrode movement or posture changes, and a Low-Pass Filter (LPF) to remove high-frequency noise like electrical interference and muscle signals (EMG). With these built-in filters, the resulting ECG signal is cleaner before being further processed by the system.

2.8. Bandpass Filter Implementation

The second method implemented for noise reduction is a Bandpass Filter (BPF) with a frequency range of 0.5-40 Hz. This filter is used to process ECG signals by only passing relevant frequencies between 0.5 Hz to 40 Hz, while eliminating frequencies below 0.5 Hz (baseline wander) and above 40 Hz (muscle noise and electrical interference). With the Bandpass Filter, the PQRST signal becomes clearer, R-peak detection is more accurate, and it improves the reliability of Heart rate variability (HRV) and VO₂Max calculations.

Specifications of the Bandpass Filter used:

- a. Lower Cutoff Frequency: 0.5 Hz
- b. Upper Cutoff Frequency: 40 Hz

2.9. Moving Average Filter (MA)

The third method used for noise reduction is the Moving Average (MA) filter with a 26-sample window. This filter works by averaging several recent samples to smooth the signal and reduce small random disturbances. With the MA filter, minor variations caused by electrical noise or electrode movement can be reduced without altering the original ECG waveform shape. This filtering approach has been widely applied in biomedical signal processing because of its simplicity and efficiency, and recent studies confirmed its effectiveness in ECG enhancement, particularly when integrated with adaptive or hybrid techniques [35], [36].

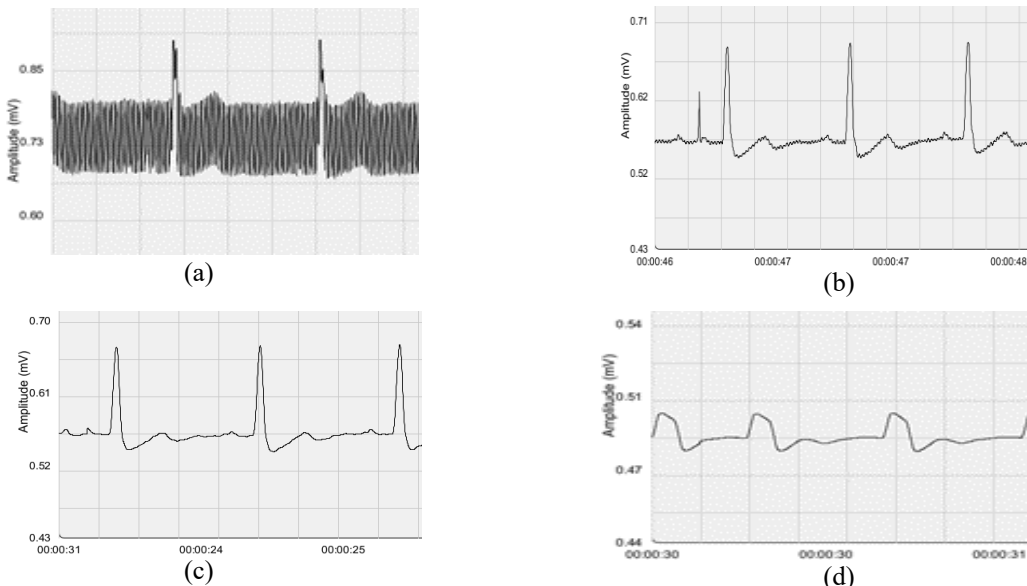


Figure 1 - (a) Original Signal; (b) Moving Average Filter 8; (c) Moving Average Filter 26; (d) Moving Average Filter 101

2.10. Data Acquisition Process

In this system, the data acquisition process is performed to obtain Electrocardiogram (ECG) signals in real-time, which are then used for Heart rate variability (HRV) and Maximal Oxygen Volume (VO₂Max) calculations. This process consists of several stages, from reading signals by the sensor to data storage and analysis.

Here are the data acquisition stages in this system:

a. Sampling Rate

The system uses a sampling rate of 1000 Hz, meaning data is collected every 1 millisecond. This frequency is chosen to capture all ECG signal details clearly, as human ECG signals have a frequency range between 0.5-40 Hz. With this sampling rate, the system ensures no important information is lost during signal recording.

b. Reading Signals from the AD8232 Sensor

The AD8232 sensor captures the heart's electrical activity through electrodes attached to the user's body. This signal is sent to Arduino Nano via pin A0, then converted from analog to digital using ADC (Analog-to-Digital Converter). This process ensures the data sent to the computer is detailed enough for further analysis.

c. Filtering to Remove Noise

After receiving the signal, the system applies a Bandpass Filter (0.5-40 Hz) to eliminate noise from electrode movement, muscle signals (EMG), and electrical interference. Additionally, the system also uses a Moving Average Filter with a 20-sample window to smooth the signal and reduce small random disturbances that may appear.

d. R-Peak Detection and HRV Calculation

After the filtering process, the system detects R-peaks in the ECG signal. This detection is important because the distance between R-peaks (R-R Interval) is used to determine Time Domain HRV. From this data, the system calculates several HRV parameters, such as SDNN, RMSSD, NN50, and pNN50, which provide information about the user's heart rate variability.

e. VO₂Max Calculation

After obtaining HRV data, the system calculates Maximal Oxygen Volume (VO₂Max) based on age, weight, automatically populated Resting Heart Rate (RHR) through the program, and automatically populated Maximum Heart Rate (MHR) when the user enters their age. This calculation is used to assess the user's aerobic capacity and physical fitness level.

f. Block Diagram System

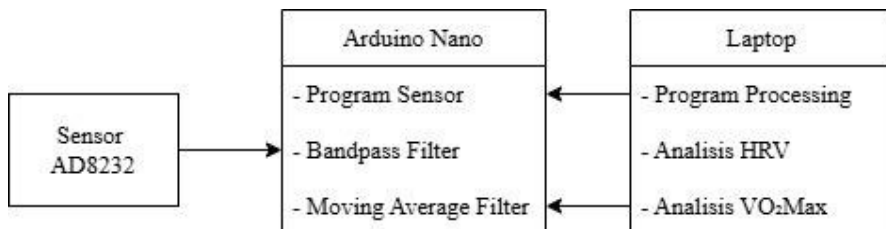


Figure 2 - Block Diagram System

The system block diagram is shown in **Figure 2**. This system consists of three main components: an AD8232 ECG sensor, an Arduino Nano microcontroller, and a computer (laptop) running Processing software. The system functions to measure Electrocardiogram (ECG) signals from the body, process data in real-time, and analyze Heart rate variability (HRV) and Maximal Oxygen Volume (VO₂Max). The AD8232 sensor functions to capture electrical signals from the heart. These ECG signals are then sent to the microcontroller for further processing. The AD8232 has high-sensitivity signal acquisition capability, enabling the system to obtain accurate and stable data. The Arduino Nano (IDE) serves as the initial processor for ECG signals received from the AD8232 sensor. The Arduino Nano uses a reader program written in Arduino IDE to read ECG signals, apply bandpass and moving average filters, before transmitting raw signals to the computer via serial communication. The Arduino Nano was selected due to its compact size and ability to handle signals in real-time. The laptop (Processing) is used to receive data from the Arduino Nano sent to the laptop running the Processing software. Processing is used for further data processing, sending start/stop commands to the Arduino, and displaying ECG signal visualization along with HRV and VO₂Max calculations. The laptop also serves as the control center and storage for analysis results that users can utilize for real-time fitness monitoring.

g. System Flowchart

In **Figure 3**, the complete system flowchart illustrates the workflow of the physical fitness monitoring system utilizing the AD8232 ECG sensor and an Arduino device. The process begins with the initialization of the graphical user interface (GUI) and all necessary variables required for system operation. Subsequently, the system opens the serial port to establish communication between the Arduino and the Processing 4 application. Once the connection is established, the system starts acquiring ECG data from the sensor. The acquired signals are processed using a bandpass filter and a Moving Average filter to remove noise and artifacts, ensuring cleaner and more reliable data. This filtering step is crucial to guarantee that the information presented to the user accurately reflects their heart activity.

Following signal processing, the data is transmitted via serial communication to the Processing 4 application, where the ECG waveform is displayed in real time. This allows users to monitor their heart rate instantly, offering immediate insight into their physiological condition. The system is also capable of detecting R-wave peaks in the ECG waveform, which are essential for calculating heart rate and heart rate variability (HRV)—both key indicators of cardiac health and the body's stress response. Additionally, users can input personal data to calculate $VO_2\text{Max}$, a widely recognized metric for aerobic capacity and cardiovascular efficiency. Upon completion of measurements, HRV and $VO_2\text{Max}$ results are automatically stored in CSV format for subsequent analysis.

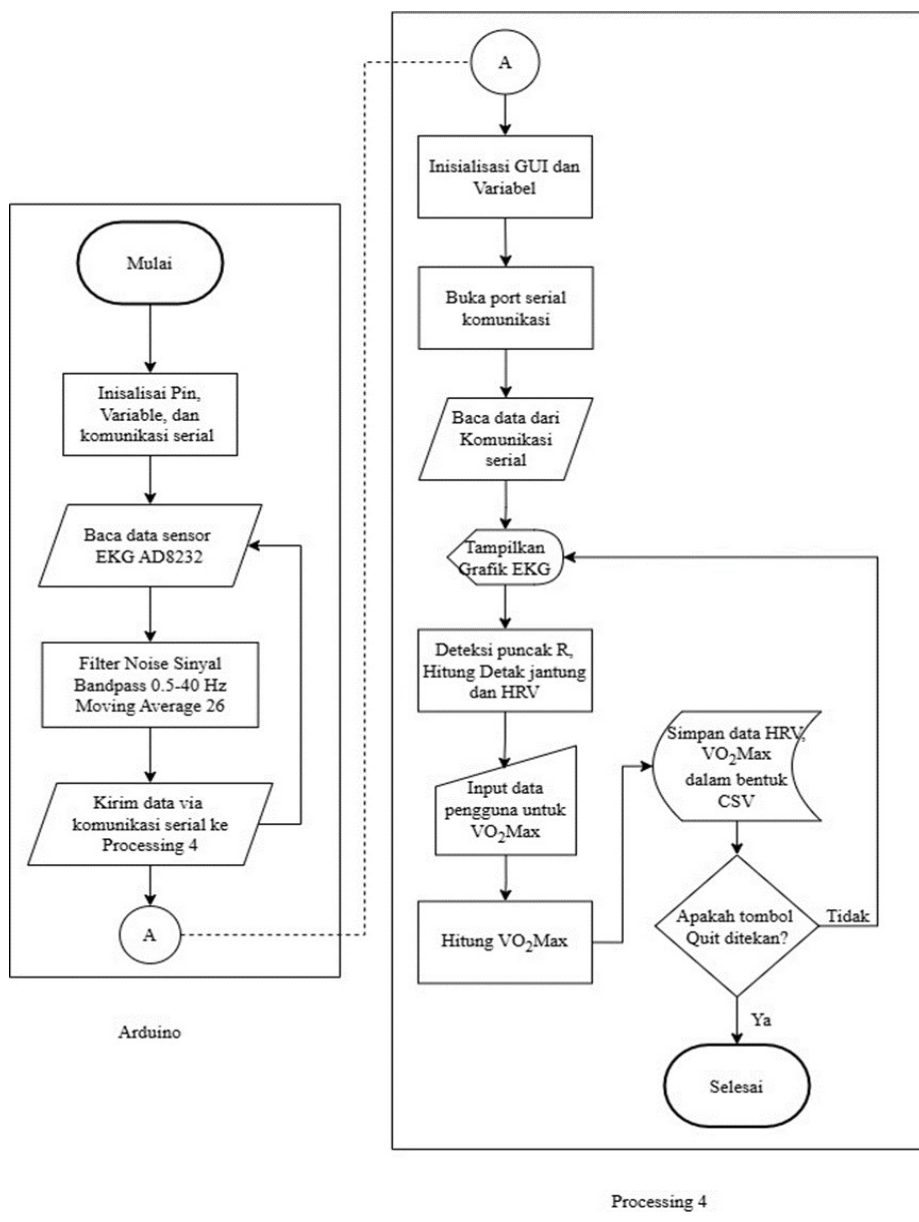


Figure 3 - System Flowchart

3. RESULT AND DISCUSSION

This study tested the designed electrocardiogram (ECG) system, which uses an Arduino Nano and an AD8232 sensor. The goal was to check how well the system could measure and analyze ECG signals from several subjects. Testing began by recording ECG signals from subjects in different physical conditions. Before each measurement, the subjects rested for a few minutes to ensure the data represented their normal condition. The ECG signals were then sent to the Processing 4 software for filtering, display, and analysis.

The test looked at how fast and accurately the system was in calculating heart rate, R-R interval, and heart rate variability (HRV). To confirm the results, measurements were also taken with a standard pulse oximeter for comparison. This step was important to see if the system could still work well in real conditions, where noise and signal changes might affect the data. The results showed that the ECG system gave accurate and reliable readings, making it suitable for monitoring physical fitness and heart health.

3.1. Electrocardiogram system testing

The Electrocardiogram (ECG) signal system was tested to evaluate its performance under different environmental and physiological conditions. Testing was carried out in two scenarios. The first scenario involved measurements in a quiet environment, free from electrical interference and excessive body movement, to obtain clean ECG signals. The second scenario involved measurements taken after subjects performed physical activities, such as using an Air Walker exercise machine or walking, to observe ECG changes caused by physical exertion. Five subjects participated in the test, with each session lasting five minutes. During this time, ECG signals were recorded, analyzed, and displayed graphically using the Processing application. **Figure 4** shows the two testing conditions: (a) a stationary or resting state, and (b) an active state after physical activity.



(a)



(b)

Figure 4 - (a) Idle condition and (b) Moving condition

In the resting condition, ECG signals were generally more stable and less affected by interference, allowing for more accurate analysis of heart rate and HRV. In the active condition, signal noise and variation increased, which could affect accuracy. Testing under both conditions demonstrated the system's ability to reliably capture and process ECG signals in real-world scenarios, whether the subject was at rest or engaged in physical activity. This comparative observation reinforces the robustness and adaptability of the developed ECG measurement system in handling diverse physiological states without significant degradation in signal quality.

Figures 5 and 6 present examples of ECG signal outputs captured during the two different testing conditions described earlier. **Figure 5** illustrates an ECG waveform obtained from a subject in a resting state. The waveform appears stable, with clearly distinguishable R-wave peaks and minimal noise interference, enabling precise calculations of heart rate and

heart rate variability (HRV). Conversely, **Figure 6** displays the ECG waveform recorded after the subject engaged in physical activity. In this condition, the waveform shows slight variations in baseline stability and increased minor fluctuations, which can be attributed to muscle activity and movement artifacts during or immediately after exercise.

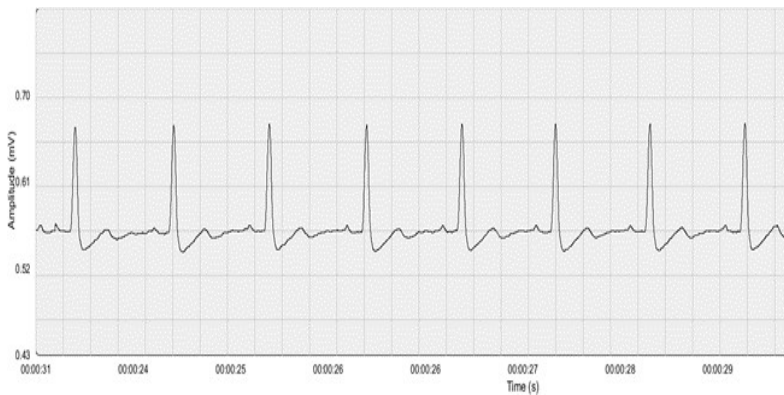


Figure 5 - Signal at rest condition

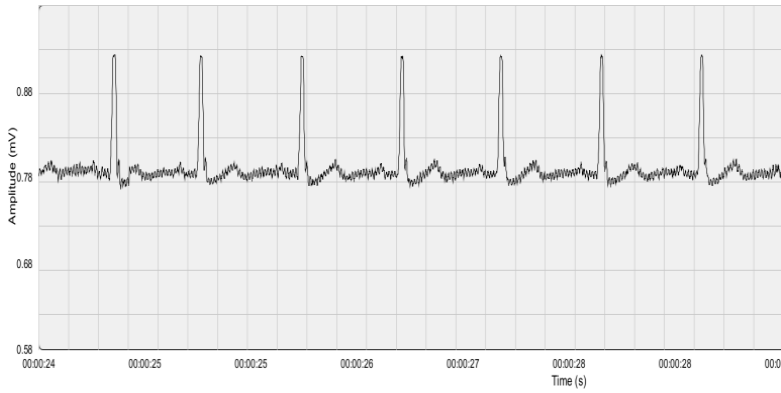


Figure 6 - Signal when moving condition

3.2. HRV and VO₂Max data collection

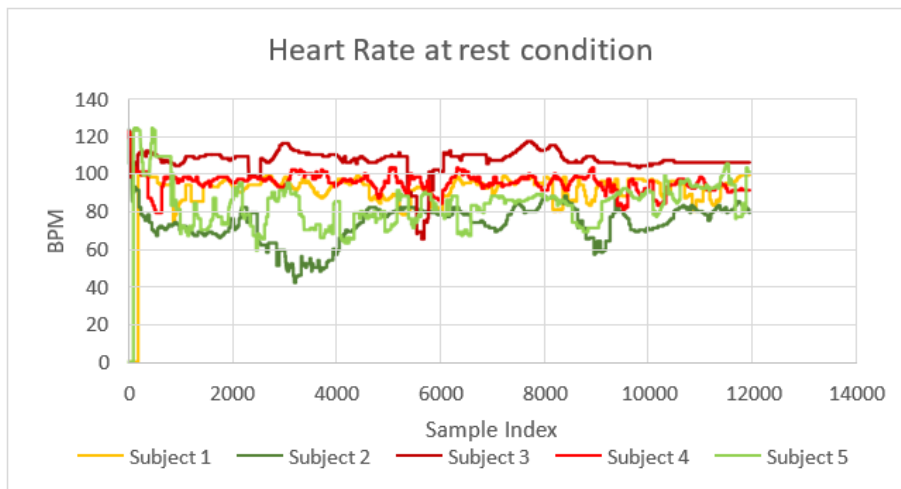
Table 1 presents the Heart Rate Variability (HRV) and Maximum Oxygen Volume (VO₂Max) measurements for five respondents (Subject 1–5), aged 20–22 years, recorded under resting and active conditions. As expected, heart rate (HR) increased during activity—for example, Subject 1's HR rose from 91 BPM at rest to 102 BPM during movement—reflecting the normal physiological response to meet increased oxygen demand. Correspondingly, the R-R interval decreased, as seen in Subject 5's data (0.68 s to 0.59 s), indicating an increased heart rate frequency. High RMSSD values, such as Subject 5's 99.76 ms at rest, signify parasympathetic dominance and a relaxed physiological state, whereas reduced values during activity suggest elevated physiological stress or exertion. SDNN, representing total heart rate variability, reflects autonomic nervous system adaptability; for instance, Subject 2's high SDNN of 129.06 ms during activity indicates strong adaptability, while Subject 4's lower value of 65.7 ms at rest suggests reduced variability and potentially lower fitness.

NN50 and pNN50 quantify the number and percentage of significant changes between consecutive heartbeats, with higher values indicating a more responsive cardiovascular system. Subject 2's pNN50 of 78% during activity demonstrates stable heart regulation, whereas Subject 5's lower value of 23.14% suggests a reduced variability response under physical load. For SD1 and SD2, higher values reflect greater stability and health in short-term and long-term heart rate patterns, respectively. Subject 5's SD1 of 169.73 ms at rest indicates strong short-term rhythm stability, while Subject 2's SD2 of 150.88 ms reflects robust long-term variability. VO₂Max, a primary indicator of aerobic capacity, follows a similar trend—the higher the value, the better the cardiovascular fitness. Subject 2 achieved the highest VO₂Max (39.9 ml/kg/min), suggesting excellent aerobic performance, whereas Subject 3 recorded the lowest (29.98 ml/kg/min), indicating relatively low aerobic capacity. These observations confirm the application's ability to accurately capture and analyze physiological changes across different activity levels, as summarized in **Table 1**.

Table 1 - HRV and VO₂Max data

Condition	Subject	Age (Years)	HR (BPM)	R-R (s)	RMSSD (ms)	SDNN (ms)	NN50	pNN50 (%)	SD1 (ms)	SD2 (ms)	VO ₂ Max (ml/kg/min)
Resting Active	Subject 1	22	91	0.64	75.36	71.87	40	66.67	64.22	73.36	32.1
			102	0.58	67.84	86.4	70	34.6	89.44	82.17	30.76
Resting Active	Subject 2	22	67	0.76	88.74	122.33	118	70	114.62	149.33	39.9
			78	0.66	76.79	129.06	129	78	126.84	150.88	38.85
Resting Active	Subject 3	20	107	0.55	93.94	62.18	23	50	56.48	55.67	29.98
			108	0.53	87.76	80.54	63	50	70.83	77.52	37.57
Resting Active	Subject 4	20	96	0.62	83.46	65.7	68	27	49.16	67.43	31.75
			94	0.63	75.03	84.76	53	28	64.71	108.68	33.73
Resting Active	Subject 5	22	85	0.68	99.76	131.88	124	77.78	169.73	135.5	37.86
			99	0.59	97.51	88.48	59	23.14	88.77	88.76	30.13

Figure 7 shows resting heart-rate traces for five study participants (Subjects 1–5). Mean resting heart rates were 91, 67, 107, 96, and 85 BPM, respectively (group mean 89.2 BPM; range 67–107 BPM; SD \approx 13.3 BPM). The data demonstrate substantial inter-individual variability: Subject 2 exhibited the lowest resting heart rate (67 BPM), consistent with superior aerobic capacity and high HRV metrics, whereas Subject 3 showed the highest resting heart rate (107 BPM) and the lowest VO₂Max in the sample, suggesting reduced aerobic fitness or acute physiological stress. These findings align with the HRV and VO₂Max results reported in **Table 1** and confirm that the developed ECG system detects meaningful between-subject differences in resting cardiovascular state. However, because the dataset is small and based on single-session recordings, further repeated and standardized measurements are recommended to fully validate these relationships.

**Figure 7 - Heart Rate at rest for the whole subject**

The data in **Figure 8** clearly show individual differences in cardiovascular responses to physical activity. Subject 1 consistently recorded the highest average heart rate (108 BPM), indicating a greater cardiovascular load during movement. This aligns with a higher resting heart rate and may suggest lower aerobic efficiency or stronger sympathetic activation. Subject 3 (102 BPM) and Subject 5 (99 BPM) also displayed relatively high average heart rates, reflecting a moderate cardiovascular demand and potentially moderate aerobic capacity. Subject 4 (94 BPM) demonstrated a moderate increase from resting conditions, indicating a balanced response to activity. In contrast, Subject 2 maintained the lowest average heart rate during movement (78 BPM), suggesting efficient cardiac performance and potentially better aerobic fitness, as supported by a high VO₂Max value and favorable HRV metrics.

From a physiological perspective, these variations in response may be due to differences in cardiovascular fitness levels, autonomic regulation, and possibly daily physical activity habits. Individuals with higher fitness levels tend to have lower heart rates at the same workload due to larger stroke volume and parasympathetic dominance. Conversely, individuals with lower physical condition or higher sympathetic nervous system dominance often exhibit a greater increase in heart rate at the same activity intensity.

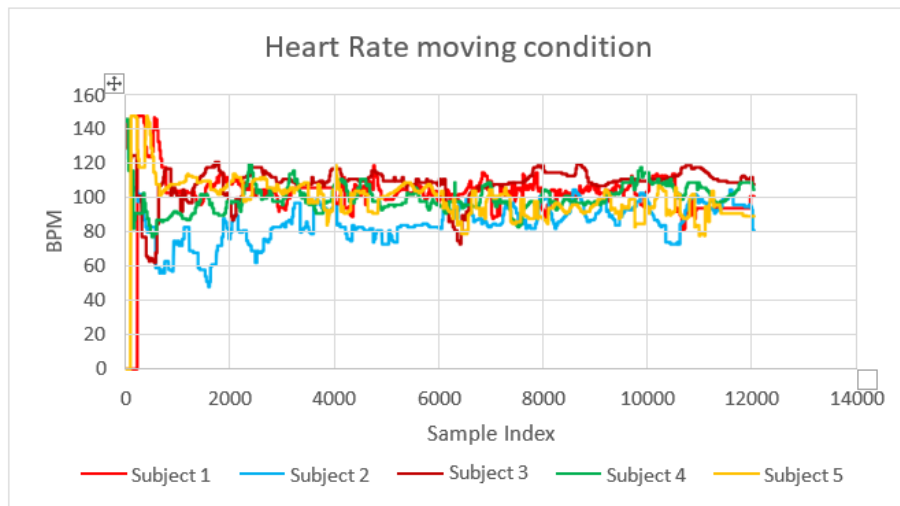


Figure 8 - Heart Rate Moving condition

The data in **Figure 9** illustrate the Root Mean Square of Successive Differences (RMSSD) values for all subjects during the resting condition, revealing notable inter-individual variability in heart rate variability (HRV). RMSSD is a time-domain HRV metric that reflects parasympathetic (vagal) activity, with higher values generally indicating greater autonomic flexibility and better cardiovascular adaptability.

Subject 2 consistently demonstrated the highest RMSSD values, peaking above 400 ms early in the measurement before stabilizing around 140–160 ms. This pattern suggests strong parasympathetic dominance at rest, which is often associated with excellent cardiovascular health and recovery capacity. Subject 1 also showed relatively high RMSSD values initially (around 300 ms), though these declined more rapidly to approximately 90–110 ms, indicating good but slightly lower vagal tone compared to Subject 2.

Subjects 4 and 3 exhibited moderate RMSSD values (70–100 ms), suggesting balanced but less pronounced parasympathetic activity. Subject 5 displayed the lowest RMSSD values throughout the resting period (approximately 60–80 ms), which may indicate reduced vagal modulation or higher baseline sympathetic tone, even at rest.

Physiologically, these differences could stem from variations in cardiovascular fitness, stress levels, sleep quality, and overall autonomic regulation. Individuals with higher RMSSD values at rest are typically better equipped to handle physical and psychological stressors, whereas lower RMSSD values may suggest limited adaptability or higher physiological strain.

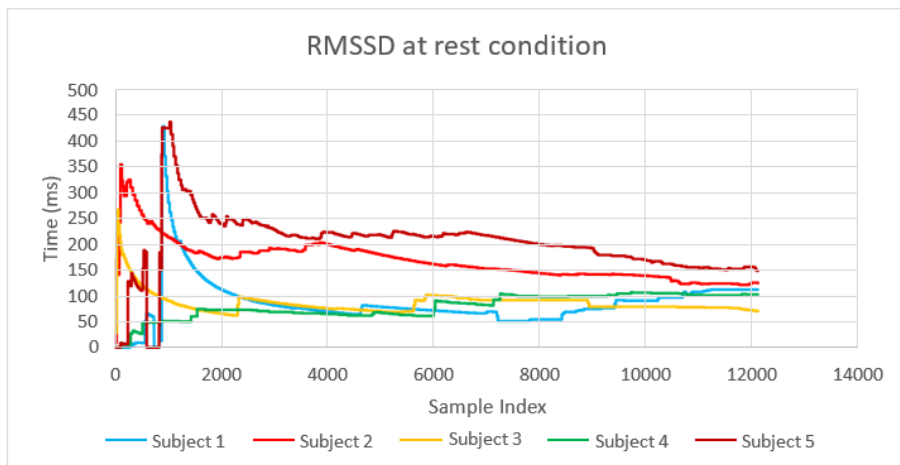


Figure 9 - RMSSD at rest Condition

Figure 10 illustrates the trend of Root Mean Square of Successive Differences (RMSSD) values for five subjects during activities with varying movement intensities. RMSSD, an established indicator of parasympathetic nervous system dominance, generally decreases as movement intensity increases or when physical fatigue occurs. In this measurement, Subject 1 recorded the highest value (97.51 ms), followed by Subject 2 (87.76 ms), indicating strong cardiovascular adaptability to physical load. Subject 3 (76.79 ms) and Subject 4 (75.03 ms) exhibited moderate responses, whereas

Subject 5 showed the lowest value (67.84 ms), which may reflect reduced parasympathetic dominance during activity. When compared with resting conditions, all subjects experienced a reduction in RMSSD—a phenomenon consistent with vagal withdrawal and a temporary shift toward sympathetic dominance as cardiovascular demands increase. Quantitatively, the absolute and percentage decreases in RMSSD (active – rest) were as follows: Subject 1: -7.52 ms (-9.98%), Subject 2: -11.95 ms (-13.47%), Subject 3: -6.18 ms (-6.58%), Subject 4: -8.43 ms (-10.10%), and Subject 5: -2.25 ms (-2.26%). The largest reduction in Subject 2 suggests high autonomic reactivity or a relatively greater perceived workload during activity, while the minimal decrease in Subject 5 indicates an ability to maintain parasympathetic tone despite movement.

Such inter-individual variations may be influenced by fitness level, physiological state at the time of measurement, and individual adaptation strategies to workload. Given that RMSSD is sensitive to analysis duration, movement artifacts, and breathing patterns, repeated measurements and standardized pre-test conditions are recommended to strengthen the validity of interpretation.

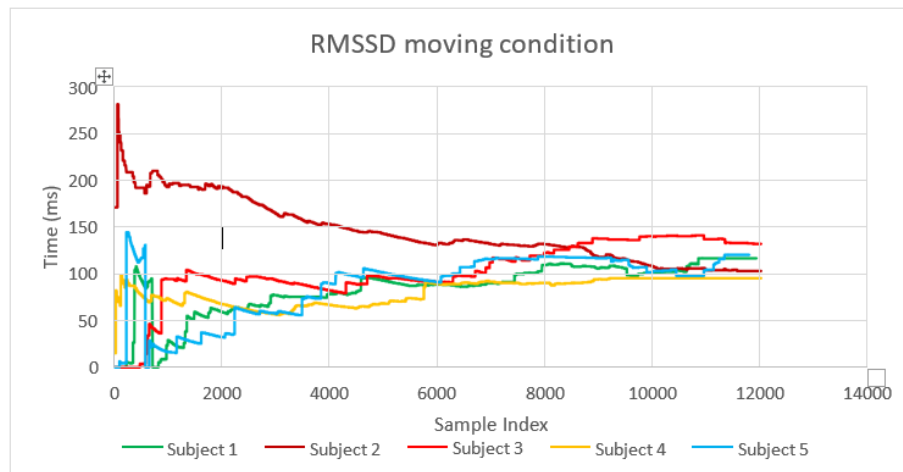


Figure 10 - RMSSD Moving Condition

In **Figure 11**, the **SDNN at rest condition** graph illustrates changes in heart rate variability (HRV) for five subjects over the measurement period. SDNN (Standard Deviation of NN intervals) reflects the extent of variation between consecutive heartbeats, where higher values generally indicate a more relaxed physiological state and better autonomic nervous system function.

At the start of the measurement, nearly all subjects exhibited relatively high and fluctuating SDNN values, likely due to the body adapting to the testing environment. Subject 1 began at approximately 200 ms and gradually decreased to around 60 ms by the end. Subject 2 recorded the highest initial SDNN of about 300 ms, which slowly declined to around 110 ms. Subject 3 started at around 80 ms and quickly stabilized at approximately 40 ms. Subject 4 began at about 120 ms and maintained a mid-range value of 80–100 ms throughout. Subject 5 also had a high initial value of around 300 ms, which gradually decreased to about 100 ms.

Over time, SDNN values for most subjects decreased and stabilized, indicating that the body had reached a steady rest condition. Subjects 2 and 5 maintained relatively high SDNN values until the end, suggesting good relaxation levels and healthy autonomic regulation. In contrast, Subject 3 had the lowest SDNN values, which may indicate a rapid relaxation response but with lower heart rate variability. These differences highlight individual variations in physiological response even under the same resting conditions.

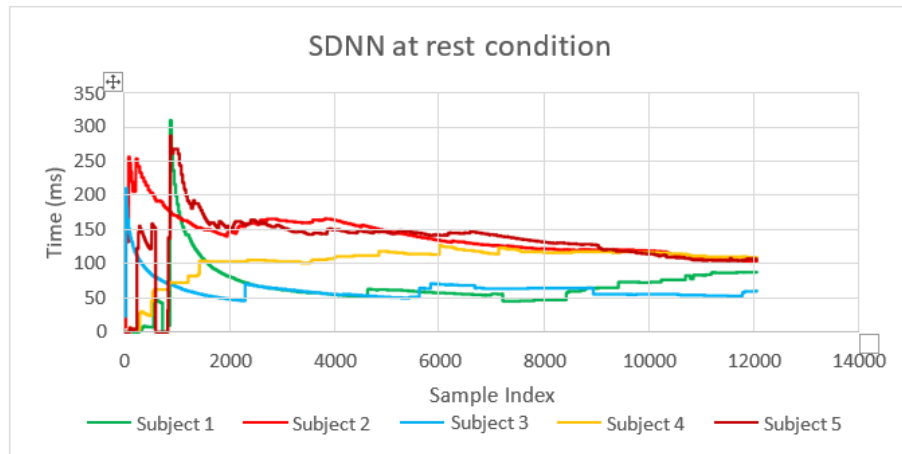


Figure 11 - SDNN at Rest Condition

In **Figure 12**, the SDNN graph under moving conditions shows the changes in heart rate variability (HRV) for five subjects throughout the measurement period. Similar to the resting condition, SDNN (Standard Deviation of NN intervals) reflects the degree of variation between consecutive heartbeats; however, under moving conditions, the values are also influenced by increased physical activity and the autonomic nervous system's response to the body's workload. At the beginning of the measurement, Subject 2 recorded the highest value at around 320 ms, which then gradually decreased to approximately 120 ms by the end, indicating the ability to maintain heart rate variability despite ongoing activity. Subject 1 started with a low value of about 50 ms but gradually increased to approximately 150 ms by the end, suggesting improved adaptation to physical activity. Subject 3 displayed a pattern similar to Subject 1, starting low at around 60 ms and increasing to about 150 ms toward the end. Subject 4 maintained a low value in the range of 50–70 ms throughout the measurement, which may indicate a lower parasympathetic response or sympathetic dominance during movement. Subject 5 also started with a low value and gradually increased to around 150 ms by the end.

Overall, this pattern shows that some subjects (1, 3, and 5) experienced an **increase in SDNN over time while moving**, indicating good physiological adaptation to activity. In contrast, Subject 4 maintained low SDNN values, while Subject 2 started with very high values but experienced a gradual decline. These differences suggest that the autonomic nervous system's response to physical activity varies among individuals, influenced by physical condition, fitness level, and the body's adaptation strategies.

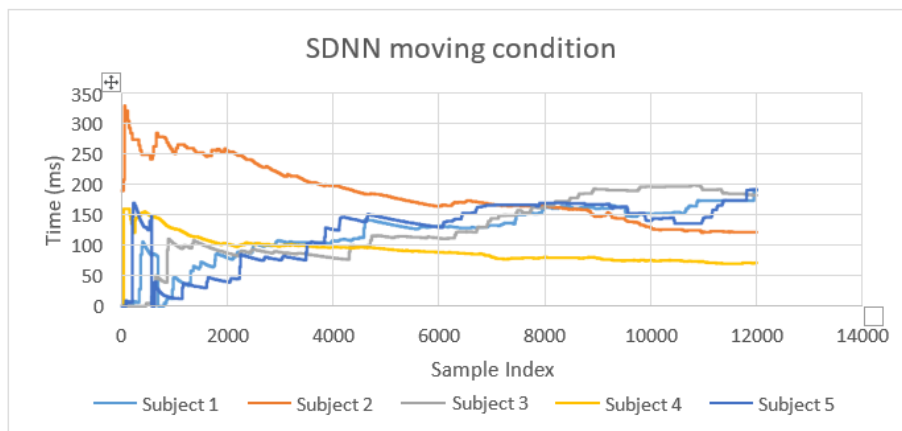


Figure 12 - SDNN Moving Condition

In **Figure 13**, the **NN50 at rest condition** graph shows the cumulative number of heartbeat interval pairs (NN intervals) that differ by more than 50 ms for five subjects during the measurement period. NN50 is a time-domain parameter of Heart Rate Variability (HRV) closely related to parasympathetic activity; higher values generally indicate better autonomic nervous system function and a more relaxed physiological state.

From the graph, Subject 5 recorded the highest value, reaching approximately 120 by the end of the measurement, followed by Subject 2 with a final value of around 100. These two subjects demonstrated high heart rate variability during rest. Subject 4 showed moderate variability with a final value of about 55, followed by Subject 3 with approximately 35. Subject 1 had the lowest value, only around 15 at the end, indicating low heart rate variability during rest.

The upward trend in NN50 for most subjects remained relatively consistent over time, suggesting that heartbeat fluctuations persisted even under resting conditions. However, the considerable differences between subjects indicate individual variations in autonomic nervous system responses, which may be influenced by factors such as cardiovascular fitness, stress levels, and lifestyle habits.

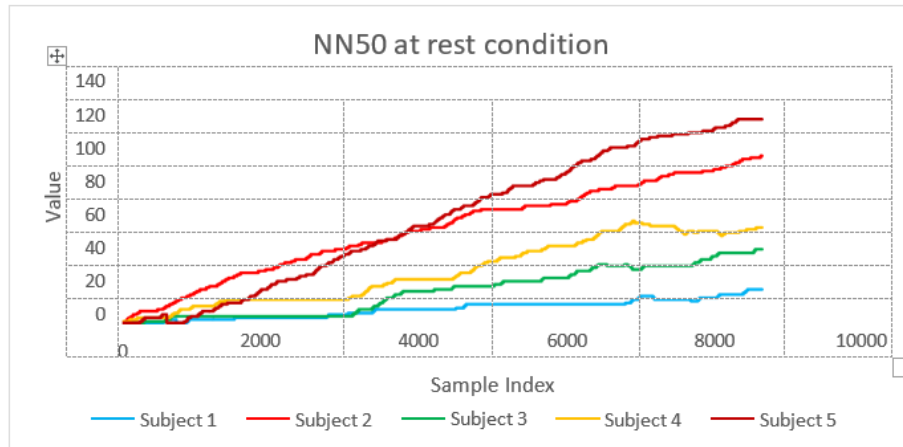


Figure 13 - NN50 at Rest Condition

In **Figure 14**, the **NN50 moving condition** graph shows the cumulative number of heartbeat interval pairs differing by more than 50 ms for five subjects while in motion. Since NN50 reflects parasympathetic activity, changes in its values during movement can indicate how the autonomic nervous system responds to physical exertion.

Subject 2 recorded the highest NN50 value, reaching approximately 125 by the end, followed closely by Subject 5 with around 110. These results suggest that both subjects maintained relatively high heart rate variability despite physical activity, indicating a strong parasympathetic influence or efficient cardiovascular adaptation. Subject 4 showed a moderate increase, ending near 80, while Subject 3 peaked around 55 before slightly declining toward the end, possibly due to fatigue or reduced parasympathetic activity. Subject 1 exhibited a steady increase throughout, finishing close to 70. Overall, the data show that most subjects experienced a progressive rise in NN50 during movement, though the rates and final values varied significantly. These differences highlight individual variations in physiological adaptation to physical activity, potentially influenced by factors such as fitness level, endurance capacity, and autonomic balance.

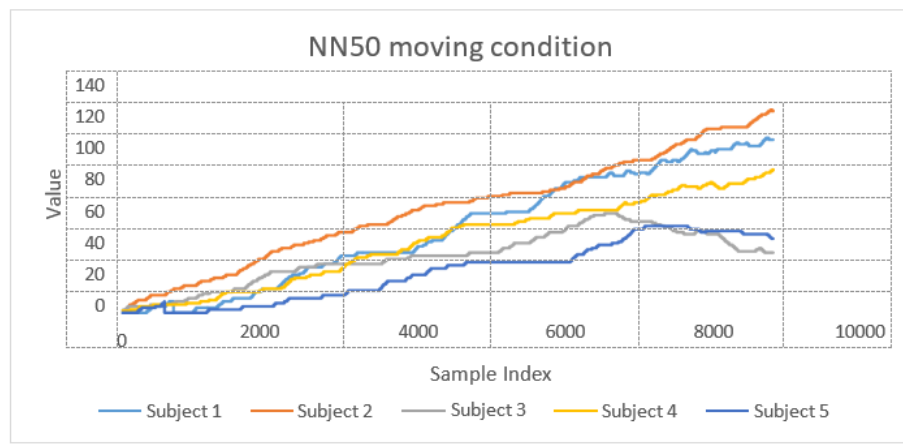
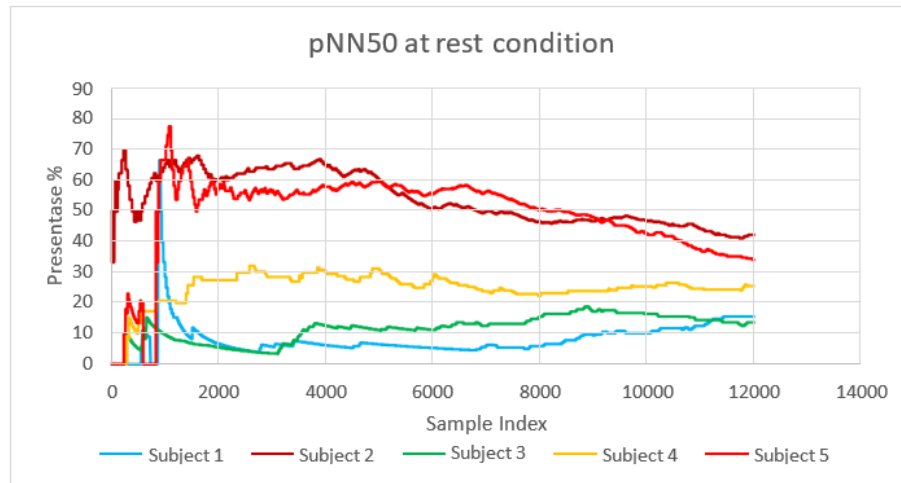
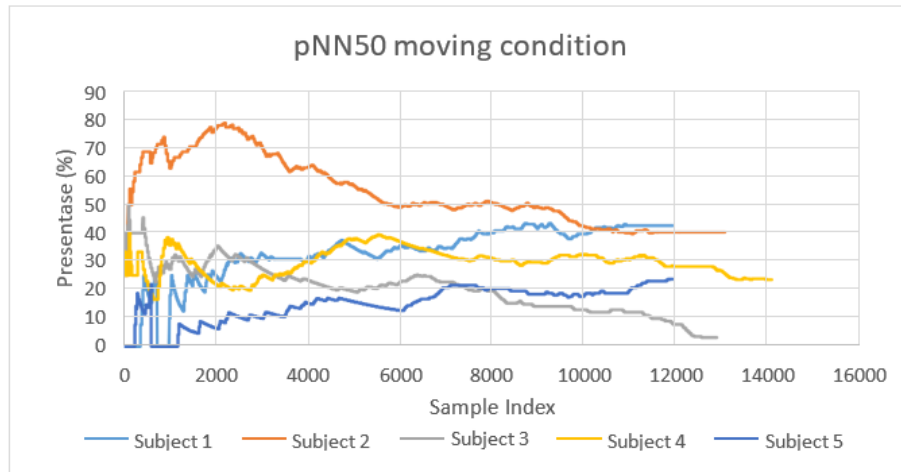


Figure 14 - NN50 Moving Condition

In **Figure 15 – pNN50 at rest condition**, the pNN50 values show clear differences among the five subjects. Subject 2 (red) starts at a high value of around 70%, maintaining between 50–70% for most of the measurement before gradually declining to about 35–40% toward the end. This indicates consistently high heart rate variability during rest. Subject 4 (yellow) maintains a moderate level around 25–30% throughout, showing stable parasympathetic activity. Subjects 3 (green) and 1 (light blue) remain at low values, generally under 15%, with a slight increase toward the end for Subject 1. Subject 5 (dark red) follows a similar trend to Subject 2 but with slightly lower values, maintaining between 40–60%. Overall, the data suggest that Subject 2 and 5 have the highest variability at rest, Subject 4 has moderate variability, and Subjects 1 and 3 exhibit lower variability, potentially reflecting differences in baseline autonomic regulation.

Figure 15 - $p\text{NN}50$ at rest condition

In **Figure 15**, during movement, $p\text{NN}50$ values decrease for most subjects compared to rest, as expected due to increased sympathetic dominance. Subject 2 maintains the highest values, peaking at around 75% in the early phase and stabilizing between 40–55% afterward. Subject 4 stays relatively stable between 25–35%, showing consistent but moderate variability. Subject 3 begins near 40% but declines steadily to below 10% by the end, suggesting reduced parasympathetic influence with prolonged activity. Subject 5 starts low but rises to around 40–45% mid-session, maintaining this level afterward. Subject 1 stays at lower levels initially but gradually increases to around 40% toward the end, indicating a delayed adaptive response to movement. In summary, movement reduces variability in most subjects, but the extent of reduction varies with Subject 2 maintaining high values throughout, and Subject 3 showing the sharpest decline.

Figure 16 - $p\text{NN}50$ Moving Condition

3.3. User Interface Testing

User interface testing confirmed that the developed ECG application provides clear and informative feedback to users through various pop-up notifications. The system successfully issues warning messages when the device is not connected and offers easily accessible user guides, complete with electrode placement illustrations and key operational notes. Upon completion of measurements, the application generates a diagnostic pop-up presenting detailed ECG analysis results—such as heart rate, R-R interval, and VO_2Max , along with user-friendly interpretations. The Start, Stop, Refresh, and Quit buttons performed as intended, enabling measurement control, real-time data updates, and safe application termination. The application also displays heart rate variability (HRV) parameters, including SDNN, RMSSD, NN50, and $p\text{NN}50$, in real time. Furthermore, the Poincaré plot visualization feature operates as expected, offering a visual representation of HRV dynamics to support data interpretation. Collectively, these features enhance the usability, reliability, and analytical capabilities of the ECG application for physical fitness monitoring and cardiac health assessment, as illustrated in **Figure 17**.

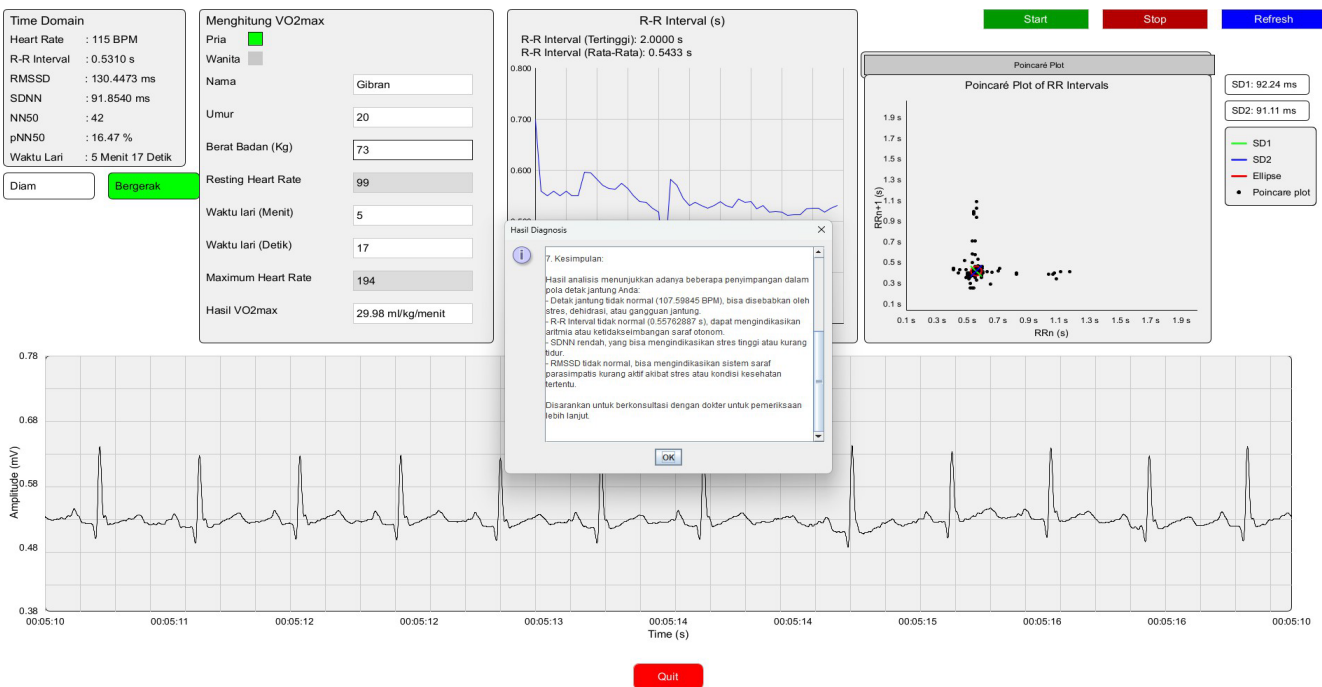


Figure 17 – User interface system

4. CONCLUSION

Testing of the ECG monitoring system based on the AD8232 sensor and Arduino Nano on five subjects (aged 20–22 years) demonstrated its ability to acquire and analyze HRV parameters in real time with stable operation for over 40 minutes. The average heart rate (HR) increased from rest to activity by $6.56\% \pm 4.8\%$, with the largest increase in Subject 1 (+12.09%) and the smallest in Subject 3 (+0.93%). Resting RMSSD values ranged from 75.36–99.76 ms and decreased by an average of $6.21\% \pm 4.7\%$ during activity, with the greatest drop in Subject 2 (-13.47%) and the smallest in Subject 5 (-2.26%). Resting SDNN values ranged from 62.18–131.88 ms, with Subject 2 showing an increase during activity (122.33→129.06 ms) and Subject 5 showing a significant decrease (131.88→88.48 ms). At rest, NN50 reached a maximum of 124 counts (pNN50=77.78%) and a minimum of 23 counts (pNN50=27%), with an average pNN50 reduction of $-18.42\% \pm 21.5\%$ during activity; the largest drop occurred in Subject 5 (-54.64%), while Subject 1 showed an increase (+26.07%). VO₂Max values were highest in Subject 2 (39.90 ml/kg/min, excellent) and lowest in Subject 3 (29.98 ml/kg/min, poor). These results confirm that the system can quantitatively differentiate physiological responses between individuals, where those with higher VO₂Max tend to have greater HRV and more controlled parasympathetic reduction during activity, while those with lower VO₂Max exhibit lower HRV, higher resting HR, and a sharp decline in pNN50 when moving. Furthermore, the observed patterns reinforce the potential of the proposed system to provide meaningful insights into individual cardiovascular fitness and autonomic regulation during exercise.

REFERENCES

- [1] C. Rachmawati, S. Martini, and K. D. Artanti, "Analisis Faktor Risiko Modifikasi Penyakit Jantung Koroner Di RSU Haji Surabaya Tahun 2019," *Media Gizi Kesmas*, vol. 10, no. 1, p. 47, 2021, doi: 10.20473/mgk.v10i1.2021.47-55.
- [2] L. Bachtiar, R. A. Gustaman, S. Mayawati, P. K. Masyarakat, I. Kesehatan, and U. Siliwangi, "Faktor Risiko Yang Berhubungan Dengan Kejadian Penyakit Jantung Koroner (PJK) (Analisis Data Sekunder di Rumah Sakit Umum Daerah Kabupaten Subang)," *J. Kesehat. komunitas Indones.*, vol. 19, no. 1, p. 52, 2023, [Online]. Available: <https://jurnal.uns.ac.id/index.php/jkki/article/view/6862>
- [3] A. Foresta, A. Setiawan, D. Ardyanto, and N. Hasanah, "Heartbeat prediction based on LSTM model on Raspberry Pi," *J. Teknol. Inf. dan Ilmu Komput.*, vol. 10, no. 7, pp. 1555–1562, 2023, doi: 10.25126/jtki.2024118015..
- [4] S. Akbar, N. Wahyu, R. Aviando, F. S. Pribadi, and R. A. Aprilianto, "Pengembangan intelligent electrocardiograph portable untuk pemantauan detak jantung: Systematic literature review," *J. Sist. Komput. dan Inform.*, vol. 9, no. 2, pp. 814–822, 2024..
- [5] H. Nissa and A. S. Rachman, "Rancang bangun alat monitoring elektrokardiogram (ECG) portabel berbasis Arduino," *TESLA: Jurnal Teknik Elektro*, vol. 26, no. 1, pp. 11–20, 2024.
- [6] K. Sangeethalakshmi, U. Preethi, S. Pavithra, and V. Shanmuga Priya, "Patient health monitoring system using IoT," *Materials Today: Proceedings*, vol. 80, pp. 2228–2231, 2023.
- [7] E. R. Ramlan Bugis, A. C. Nur'Aidha, and D. Y. H. Kumaraqati, "Alat Monitoring Detak Jantung Portable Menggunakan Sensor Max30102," *J. Inform. dan Tek. Elektro Terap.*, vol. 12, no. 3, 2024, doi: 10.23960/jitet.v12i3.4504.
- [8] R. Royan, "Studi Akurasi Sensor ECG AD8232 Terhadap ECG Simulator," *Cyclotron*, vol. 7, no. 02, pp. 48–51, 2024, doi: 10.30651/cl.v7i02.23095.
- [9] V. Dange, S. Ruikar, S. Kadam, R. Sidanale, S. Sangwai, and S. Sadake, "Portable ECG monitoring system using AD8232 and ESP8266," in *Proc. 2024 Int. Conf. Artif. Intell. Quantum Comput.-Based Sensor Appl. (ICAQSA)*, Dec. 2024, pp. 1–6.

[10] M. R. Pamungkas, "Monitoring heart rate, ECG, dan SpO2 untuk aktivitas treadmill," Doctoral dissertation, Universitas Muhammadiyah Yogyakarta, 2024.

[11] T. Möller, Y. Georgie, M. Voss, and K. Kaltwasser, "An Arduino-based heartbeat detection device (ArdMob-ECG) for real-time ECG analysis," in *Proc. IEEE Signal Process. Med. Biol. Symp. (SPMB)*, Dec. 2022, pp. 1–3, doi: 10.1109/SPMB55497.2022.10014819.

[12] S. K. Nayak et al., "A Review of Methods and Applications for a *Heart rate variability Analysis*," *Algorithms*, vol. 16, no. 9, 2023, doi: 10.3390/a16090433.

[13] Utama, J., & Aminudin, Y. M, "Design of drunk detection device using non-linear analysis of the heart rate variability method," In *AIP Conference Proceedings* (Vol. 2510, No. 1, p. 030027). AIP Publishing LLC, 2023. <https://doi.org/10.1063/5.0129267>

[14] S. Wiecha et al., "External validation of $\dot{V}O_2\text{Max}$ prediction models based on recreational and elite endurance athletes," *PLoS One*, vol. 18, no. 1 January, pp. 1–22, 2023, doi: 10.1371/journal.pone.0280897.

[15] H. Hoppeler, "Deciphering $\dot{V}O_2\text{max}$: Limits of the genetic approach," *J. Exp. Biol.*, vol. 221, no. 21, 2018, doi: 10.1242/jeb.164327

[16] R. J. McNamara, "The physiologic basis of the electrocardiogram," *W. Va. Med. J.*, vol. 45, no. 10, pp. 269–280, 1949.

[17] N. Rafie, A. H. Kashou, and P. A. Noseworthy, "ECG Interpretation: Clinical Relevance, Challenges, and Advances," *Hearts*, vol. 2, no. 4, pp. 505–513, 2021, doi: 10.3390/hearts2040039.

[18] A. Rawshani, "Methodological ECG Interpretation," *ECGwaves*, vol. pocket gui, 2017, [Online]. Available: www.ECGwaves.com%7C

[19] A. B. Mahajito and I. Handayani, "Athlete's Heart (Jantung Atlet)," *Cermin Dunia Kedokt.*, vol. 46, no. 12, pp. 732–737, 2019, [Online]. Available: <http://www.cdkjournal.com/index.php/CDK/article/view/392>

[20] M. Ehnesh, P. Abatis, and F. S. Schlindwein, "A portable electrocardiogram for real-time monitoring of cardiac signals," *SN Appl. Sci.*, vol. 2, no. 8, pp. 1–11, 2020, doi: 10.1007/s42452-020-3065-9.

[21] U. Suripto and J. Utama, "Telemonitoring elektrokardiografi portabel," *Telekontran*, vol. 2, no. 1, pp. 19–28, 2014.

[22] M. M. Corrales, B. de la C. Torres, A. G. Esquivel, M. A. G. Salazar, and J. Naranjo Orellana, "Normal values of *heart rate variability* at rest in a young, healthy and active Mexican population," *Health (Irvine. Calif.)*, vol. 04, no. 07, pp. 377–385, 2012, doi: 10.4236/health.2012.47060.

[23] J. Hart, "Optimal level of *heart rate variability* for spinal adjustment: A case report.," vol. 2, no. 1, p. Online-access only p 103-108, 2019.

[24] T. Pham, Z. J. Lau, S. H. A. Chen, and D. Makowski, "Heart rate variability in psychology: A review of *HRV* indices and an analysis tutorial," *Sensors*, vol. 21, no. 12, pp. 1–20, 2021, doi: 10.3390/s21123998.

[25] L. Rosenthal, "Normal Electrocardiography (ECG) Intervals: Normal Electrocardiography Intervals," *Medscape*, p. 2172196, 2020, [Online]. Available: <https://emedicine.medscape.com/article/2172196-overview>

[26] E. M. Tangen, C. Gjestvang, T. Stensrud, and L. A. H. Haakstad, "Is there an association between total physical activity level and $\dot{V}O_2\text{Max}$ among fitness club members? A cross-sectional study," *BMC Sports Sci. Med. Rehabil.*, vol. 14, no. 1, pp. 1–8, 2022, doi: 10.1186/s13102-022-00503-4.

[27] M. T. Hansen, K. Husted, J. L. Modvig, K. K. Lange, C. M. Weinreich, C. Tranberg, ... and J. W. Helge, "VO₂peak estimation in people with overweight and obesity before and after a 14-week lifestyle intervention: Clinical research," *Int. J. Obes.*, vol. 49, no. 5, pp. 864–871, May 2025, doi: 10.1038/s41366-025-01713-9.

[28] X. Feng, L. Zhao, Y. Chen, Z. Wang, H. Lu, and C. Wang, "Optimal type and dose of hypoxic training for improving maximal aerobic capacity in athletes: a systematic review and Bayesian model-based network meta-analysis," *Front. Physiol.*, vol. 14, no. September, pp. 1–10, 2023, doi: 10.3389/fphys.2023.1223037.

[29] H. Hov et al., "Aerobic high-intensity intervals are superior to improve $\dot{V}O_2\text{max}$ compared with sprint intervals in well-trained men," *Scand. J. Med. Sci. Sport.*, vol. 33, no. 2, pp. 146–159, 2023, doi: 10.1111/sms.14251.

[30] G. Weisstaub, J. González, I. Orizola, J. Borquez, M. Monsalves-Alvarez, L. Lera, R. Troncoso, and C. Sepúlveda, "Validity and reliability of the step test to estimate maximal oxygen consumption in pediatric population," *Sci. Rep.*, vol. 15, no. 1, Art. no. 592, 2025, doi: 10.1038/s41598-024-84336-w.

[31] M.-O. Dugas, P. Paradis-Deschênes, L. Simard, T. Chevrette, P. Blackburn, and M. Lavallière, "Comparison of $\dot{V}O_2\text{max}$ estimations for maximal and submaximal exercise tests in apparently healthy adults," *Sports*, vol. 11, no. 12, Art. no. 235, 2023, doi: 10.3390/sports11120235.

[32] G. Carrick-Ranson et al., "The effect of age-related differences in body size and composition on cardiovascular determinants of $\dot{V}O_2\text{Max}$," *Journals Gerontol. - Ser. A Biol. Sci. Med. Sci.*, vol. 68, no. 5, pp. 608–616, 2013, doi: 10.1093/gerona/gls220.

[33] A. A. Fedotov, "Selection of Parameters of Bandpass Filtering of the ECG Signal for Heart Rhythm Monitoring Systems," *Biomed. Eng. (NY)*, vol. 50, no. 2, pp. 114–118, 2016, doi: 10.1007/s10527-016-9600-8.

[34] B. Hall, S. Patel, A. Jones, and M. Wilson, "The impact of ECG filter settings on pseudo-ST elevation," *J. Am. Coll. Cardiol.*, vol. 83, no. 12, pp. 1154–1162, 2024, doi: 10.1016/j.jacc.2024.03.015.

[35] S. Banerjee and P. K. Bora, "Real-time ECG signal enhancement using moving average and adaptive filtering techniques," *Biomed. Signal Process. Control*, vol. 83, Art. no. 104623, 2023, doi: 10.1016/j.bspc.2023.104623.

[36] H. Zhang, L. Wang, Y. Chen, and M. Li, "Noise reduction in wearable ECG monitoring using moving average and wavelet-based hybrid filters," *Sensors*, vol. 23, no. 7, pp. 1–14, 2023, doi: 10.3390/s23073745.